A Novel Micropipet Method for Measuring the Bending Modulus of Vesicle Membranes

Doncho V. Zhelev, David Needham, and Robert M. Hochmuth
Department of Mechanical Engineering and Materials Science Duke University, Durham, North Carolina 27708-0300 USA

ABSTRACT A theoretical model and an experiment are presented for determining the bending modulus of a bilayer vesicle membrane. The vesicle is held with a pipet having a radius between 1 and 2 μm, and the tension in the membrane is changed by changing the suction pressure. Then the vesicle membrane is deformed by aspirating it into a smaller pipet having a radius on the order of 0.5 μm. The relationship between the suction pressures in the two pipets is found to be linear, as predicted by the theoretical model. The curvature of the vesicle membrane at the pipet orifice and the bending modulus are found with the help of the model from the slope and the intercept of the linear experimental relationship between the suction pressures in the two pipets. The bending modulus for the two SOPC membranes studied in these experiments was found to be either 0.6 or 1.15×10^{-19} J, which is similar to the values measured previously.

INTRODUCTION

The lipid bilayer membrane above the gel-liquid phase transition temperature behaves as a two-dimensional liquid that is isotropic in the plane of the membrane. However, although the membrane is a two-dimensional liquid, it has an elastic resistance to being curved or "bent" because of the differential expansion and contraction that occurs when the two liquid surfaces of the bilayer are curved (Helfrich, 1973). This bending rigidity is characterized by a bending modulus that has an inherently small value because the bilayer is so thin.

To measure the bending modulus of a membrane, it must be curved in some measurable way with known and well characterized forces or moments. There are now several methods for determining the bending modulus of lipid membranes. They can be divided into two groups: 1) zero mean tension methods and 2) nonzero mean tension methods. Zero mean tension methods are based on characterizing the thermal excitations of free lipid membranes with two different geometries: bilayer cylinders (Servuss et al., 1976; Schneider et al., 1984a) or spherical vesicles (Schneider et al., 1984b; Milner and Safran, 1987; Faucon et al., 1989; Duwe et al., 1990). Nonzero mean tension methods have been developed recently in which either the mean vesicle area at different membrane tensions is related to the thermal excitations of the vesicle surface (Evans and Rawicz, 1990) or the change of the free energy per unit area (the membrane tension) of a spherical vesicle is related to the change of the bending energy stored in a "tether" pulled from the vesicle (Waugh et al., 1992). Thermal excitation methods require a measurement of the amplitudes of the surface fluctuations and are limited to the resolution of the light microscope. A problem can arise for membranes having large surface viscosity, when high frequency surface fluctuations will be damped by the viscous dissipation in the membrane (Duwe et al., 1990). In the method in which a tether is extracted from a vesicle, the diameter of the tether is not a directly measurable parameter. Also, when working with lipid mixtures, the high curvatures produced in the tether region can lead to differences in lipid composition in the tether region and the spherical region of the vesicle, or to lipid exchange between the two monolayers. Thus, we have developed in this work another nonzero tension method that does not depend on thermal excitations and at the same time does not produce regions of large scale curvature. This method might not be as sensitive as the other methods mentioned above for measuring small bending moduli, but will be successful for measuring large bending moduli. In addition, a similar method to the one used in this paper is developed in an accompanying paper (Zhelev et al., 1993) and then used to determine the apparent bending modulus of the surface of a neutrophil.

THEORETICAL BACKGROUND

The experiment, shown in Fig. 1, is to find the pressure necessary to deform the vesicle membrane into a smaller pipet when the vesicle is aspirated into another, larger pipet. It is assumed that the shape of the vesicle surface at first approximation can be represented by various spherical segments and a cylinder and two torus segments at the orifices of the two pipets (Fig. 1 B). In the following analysis, the vesicle is divided into six regions. The change of the total vesicle free energy is calculated for small deviations of the shape of its membrane inside the small pipet relative to a hemispherical shape. Then the perturbation of the free energy is related to the corresponding work for the membrane displacements in the six regions. Because the experiments are performed above the phase transition temperature, the shear elasticity and the elastic resistance related to Gaussian cur-

Received for publication 13 October 1993 and in final form 4 May 1994.
Address reprint requests to D. V. Zhelev, Department of Mechanical Engineering and Materials Science, Duke University, Durham, NC 27708-0300. Tel.: 919-660-5353; Fax: 919-660-8963.
Dr. Zhelev's permanent address: Central Laboratory of Biophysics, Bulgarian Academy of Sciences, Sofià 1113, Bulgaria

0006-3495/94/08/720/08 $2.00

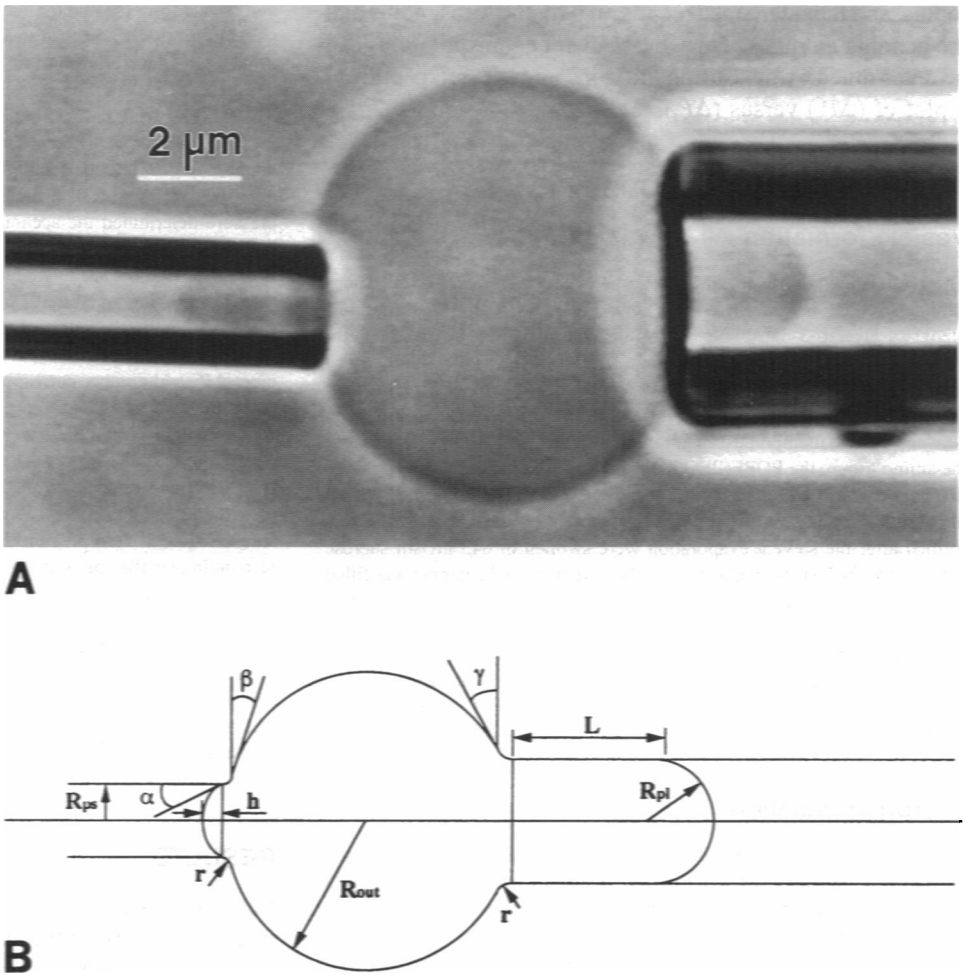

FIGURE 1 (*A*) A vesicle partially aspirated into two pipets with different pipet radii. (*B*) Schematic of the experiment showing the geometric parameters used in the model. *r* is the "small torus radius."

vature are neglected. Initially, the vesicle is held in the large pipet at a given suction pressure. The volume of the vesicle is determined by the osmotic equilibrium between the inside and outside solution, and its area depends on the applied suction pressure. When the vesicle membrane is deformed in the small pipet, its liquid interior is compressed. However, it is assumed that this additional increase in the internal pressure does not lead to volume and area changes because the dependence of the volume on the suction pressure is small (Kwok and Evans, 1981) and the area changes are negligible because of a large area compressibility modulus (Evans and Skalak, 1980). Thus, the volume and the surface area of the vesicle for a given measurement are assumed to be constant. The tension along the membrane is assumed to be constant and to be determined by the suction pressure in the large pipet. Then the bending elasticity is the only source for increasing the free energy of the vesicle during this small deformation. We define the bending energy g_b per unit vesicle area as (Helfrich, 1973)

$$g_b = \frac{k_c}{2}(c_1 + c_2)^2 \tag{1}$$

where k_c is the bending modulus, and c_1 and c_2 are the two principal curvatures. The spontaneous curvature is assumed to be zero.

The total change of the vesicle bending free energy, dG_{total}, when the projection length of its membrane in the small pipet is changed from h to $h + dh$ (for $h < R_{ps}$, where R_{ps} is the small pipet radius) is the sum of the free energy changes for all six regions (see Appendix Eq. A10). From the conservation of energy principle, this change of the free energy is equal to the work dW_{total} for displacing all nonrestricted boundaries (Eq. A13). Then from these conditions, the functional relationship between the measured suction pressures in the small (ΔP_s) and the large (ΔP_l) pipets and the geometric characteristics of the experiment are

$$\Delta P_s = f_0\left(\frac{R_{pl}}{R_{ps}}, \frac{R_{out}}{R_{ps}}, \frac{r}{R_{ps}}\right)\cdot\frac{k_c}{R_{ps}^3} + f_1\left(\frac{R_{pl}}{R_{ps}}, \frac{R_{out}}{R_{ps}}, \frac{r}{R_{ps}}\right)\cdot\frac{\Delta P_l}{R_{ps}}, \tag{2}$$

where the functional coefficients are defined in the Appendix. Briefly, R_{ps} and R_{pl} are the small and the large pipet radii, R_{out} is the outside vesicle radius, and r is the small torus radius as shown in Fig. 1 *B*.

There are only two parameters in Eq. 2 that are not known: the bending modulus k_c and the small torus radius r. The relationship between the two suction pressures is linear as predicted by Eq. 2, the slope depends only on the small torus

radius, and the intercept depends on both the torus radius and the bending modulus. Thus, the bilayer bending modulus can be determined by measuring the slope and the intercept from a plot of (ΔP_s) versus (ΔP_l).

MATERIALS AND METHODS

Vesicle formation

The vesicles were made of 1-stearoyl-2-oleoyl-*sn*-glycero-3-phosphocholine (SOPC: M_r 788.14, Avanti Polar-Lipids, AL) and 1-palmitoyl-2-oleoyl-*sn*-glycero-3-phosphoethanolamine with covalently bonded polyethylene glycol (POPE(PEG5000): average M_r 5700, Avanti Polar-Lipids). The lipid composition was SOPC:POPE(PEG5000) at a ratio of 99:1. In this way, the PEG chain, which was soluble in water, provided a steric repulsion between vesicle membranes. In addition, because the PEG was attached to the amino group, the POPE(PEG5000) molecule had a negative net charge that provided an additional electrostatic repulsion. The lipids were dissolved in chloroform, and the solvent was evaporated in nitrogen. The lipid layers formed after the solvent evaporation were swollen in 643 mOsm sucrose solution (M_r 342.3) overnight at 36°C. The experimental chamber was filled with 647 mOsm dextrose solution (M_r 180.16) with 0.15% albumin (BSA, Boehringer Mannheim, Indianapolis, IN). High osmolarities in the solutions were used to provide a sufficient difference in the refractive index between the inside and outside media. The experiments were performed at 14°C, which was the dew point for the day. (Then the rate of evaporation and condensation were the same.)

Micromanipulation

An inverted Leitz microscope with a 100× oil immersion objective was used in the experiments. The microscope images were recorded using a Hamamatsu CCD camera. The experimental chamber was 3 mm thick and open from both sides for micromanipulation. For temperature control, there was a flow of water between two glass slides on the top of the chamber. There was a temperature gradient along the chamber height that produced a small convection current. The chamber was trans-illuminated at 435 ± 4 nm, which minimized the diffraction patterns around the pipets. Micropipets were made from 0.75 mm capillary glass tubing pulled to a fine point with a vertical pipet puller. The tip of the pipet was immersed in a melted glass bead made of a glass with a lower melting temperature than the pipet. Then the bead was allowed to cool and the pipet was pulled until it broke at the desired diameter. The large and the small pipets used in the experiments had radii of 1.33 and 0.58 μm, respectively. The pipets were filled with the same solution as was in the chamber. A small number of 0.7 μm latex beads (Seradyn, Indianapolis, IN) with a high refractive index were added to the chamber. The beads were used for zeroing the pressure in the pipets and for tracing the flow in the chamber. The latex beads did not adhere to the vesicles or to the pipets. The pipets were connected to a manometer system, with which the pipet-chamber pressure difference could be varied between 0.5 and 100 Pa using the micrometer-driven displacement of a water reservoir. High pressures were measured with differential pressure transducers (Validyne DP103 and P7D) for pressure differences up to 2,000 and to 10,000 Pa, respectively. Readouts from the pressure transducers were displayed on the video image using a video multiplexer (Vista Electronics 401). After an experiment, the pipets were washed with water and chloroform several times, dried in a vacuum, and the pipet diameters were measured using a scanning electron microscope (Philips 501).

The experiments were performed with two pipets as shown in Fig. 1*A*. One, the holding pipet, had a large radius (on the order of few microns), and the other had a small radius (on the order of half a micron). The pressure in the two pipets was zeroed at the position used in the experiment, which typically was at a distance slightly larger than the vesicle radius. A single vesicle was chosen and aspirated into the large, holding pipet. The vesicle shape was spherical outside the pipet, with a cylindrical portion inside and a hemispherical cap at the end. The suction pressure in the large pipet was slightly above the pressure at which the vesicle membrane could fluctuate and escape from the pipet. Then the small pipet was positioned at the other side of the vesicle so that it touched the vesicle surface without deforming it. The pipets were not moved from this position until the end of the experiment. The suction pressure in the small pipet was increased in steps of 0.5 or 1.0 Pa every half a minute until the vesicle membrane started to flow into the small pipet. The determination of the suction pressure for vesicle membrane flow into the small pipet for a given suction pressure in the large pipet was repeated 2 or 3 times. The step size for increasing the suction pressure determined the accuracy of the measurements. Once the vesicle membrane started to flow into the small pipet, it continued flowing until the cylindrical portion inside the holding pipet disappeared. The suction pressure for initiating membrane flow was the small pipet suction pressure ΔP_s corresponding to the suction pressure ΔP_l imposed by the large pipet. The experiment was repeated by increasing the suction pressure of the holding pipet ΔP_l, and another corresponding suction pressure for initiating membrane flow into the small pipet ΔP_s was found. The "zero" of both pipets was measured during the experiment and at the end of the experiment to check for possible changes. The suction pressure for membrane flow when the vesicle was not held by the large pipet and had settled to the bottom of the experimental chamber was measured as well. This gave a suction pressure for flow at zero pressure in the holding pipet. After finding the corresponding small-pipet suction pressure for the chosen large-pipet suction pressure, the vesicle area change until lysis was measured as a function of the suction pressure in the large pipet to find the number of bilayers in the liposome by measuring its area compressibility modulus (Kwok and Evans, 1981). Only results from single bilayer vesicles were reported here. The bending modulus of the vesicle was determined both from pipet measurements made with two pipets using the theoretical model (Eq. 2) and from measurements with one pipet following the theory and method of Evans and Rawicz (1990).

RESULTS

Fig. 2 shows the measured corresponding suction pressures in the two pipets for the experiment illustrated in Fig. 1. Once the vesicle membrane was deformed into a hemispherical shape, it started to flow into the small pipet. Reducing the

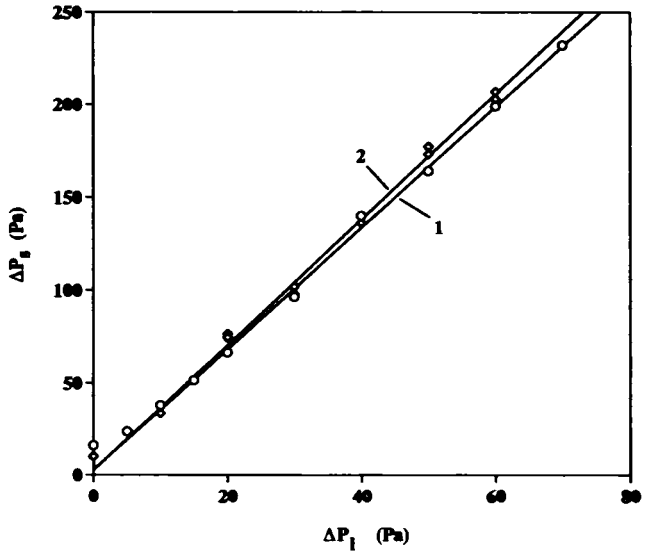

FIGURE 2 Suction pressure in the large pipet ΔP_l and the corresponding suction pressure for vesicle flow in the small pipet ΔP_s for two SOPC vesicles. The (dimensionless) slope and the intercept for the first vesicle are 3.27 and 2.87 Pa, respectively, and that for the second vesicle are 3.38 and 2.74 Pa. Only critical suction pressures ΔP_s above 30 Pa are used for determining the slopes and the intercepts.

suction pressure in the small pipet allows the vesicle to flow back into the large pipet. By manipulating the suction pressure in the small pipet a metastable equilibrium can be reached when the vesicle is partially aspirated into the two pipets as shown in Fig. 1 *A*. The pressure required for metastable equilibrium was smaller than the pressure for deformation and flow. The difference between the suction pressure necessary for deformation into the small pipet and the pressure sufficient to keep the vesicle in a position of metastable equilibrium was on the order of 2–4 Pa.

The relationship between the suction pressures in the two pipets when the vesicle started to flow into the small pipet was linear except at small suction pressures (Fig. 2). The model, as illustrated by Eq. 2, predicted a linear relationship between the two suction pressures for all suction pressures when the membrane tension in the nondeformed (free) vesicle was zero. It was assumed that the nonlinearity for small suction pressures of the holding pipet was caused by the existence of a nonzero membrane tension in the free vesicle primarily because of thermal fluctuations of the membrane. The measured suction pressures in the small pipet at zero suction pressure in the large pipet were 10 and 16 Pa for the two vesicles studied here. The corresponding "true" suction pressures of the large pipet found from the regression line (the regression line was for the data with ΔP_s greater than 30 Pa) were 2.5 Pa and 4 Pa, respectively. An outside vesicle radius of 3.36 or 4.19 μm and a large pipet radius of a 1.33 μm gives an effective membrane tension on the order of $2.8–3.9 \times 10^{-3}$ mN/m. Another estimation of the membrane tension of a free vesicle was found from the suction pressure at which the vesicle membrane started to fluctuate and to escape from the large pipet. The vesicles studied here started to fluctuate at suction pressures between 2 and 2.5 Pa. The corresponding effective membrane tensions were $2.2–2.8 \times 10^{-3}$ mN/m.

The (dimensionless) slopes and the intercepts determined from Fig. 2 for the two vesicles were 3.27 and 2.87 Pa, respectively, for the first vesicle and 3.38 and 2.74 Pa for the second one. The slope from Eq. 2 was a function only of the small torus radius, but not of the bending modulus. Then the small torus radii corresponding to these slopes were 0.125 μm for the first and 0.09 μm for the second vesicle. These estimates for the small torus radii and the intercepts from the regression lines, when used with Eq. 2, gave values for the bending moduli of 0.72×10^{-19} and 0.58×10^{-19} J for the two vesicles studied.

Single pipet measurements of the dependence of the membrane tension on fractional area expansion are shown in Fig. 3. The dependence between the induced membrane tension and the fractional area expansion was not linear for low tensions, because part of the applied suction pressure went for smoothing the amplitudes of the thermal fluctuations. For large membrane tensions, when the amplitudes of the thermal fluctuations were practically zero, the dependence was linear and the relative area changes were caused only by an increase in the total surface area (or area per lipid molecule). The slope in this case gave an estimate for the area expansion modulus (Kwok and Evans, 1981). In these experiments, the area expansion modulus for one of the vesicles was 182 mN/m and for the other was 178 mN/m. The area expansion modulus for SOPC bilayers as measured by Evans and Rawicz (1990) was 190 mN/m. This showed that single bilayer vesicles were used in these experiments. The bending moduli for the same two vesicles found from the dependence of the logarithm of the membrane tension on the relative area expansion at small tensions (Fig. 4), were 1.1×10^{-19} and 0.7×10^{-19} J for the first and the second vesicle, respectively. Using this method, Evans and Rawicz (1990) reported a value 0.9×10^{-19} J for SOPC bilayers.

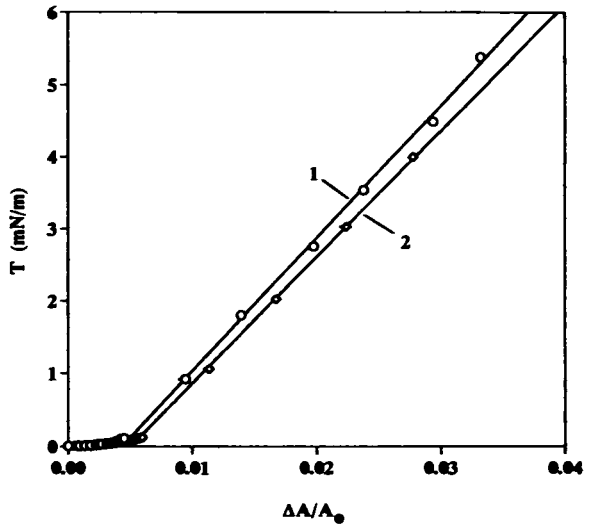

FIGURE 3 Membrane tension versus the relative fractional area change for the vesicles shown in Fig. 2. The dependence is linear for large suction pressures, and the slope in this domain, which represents the area expansion modulus, is 182 mN/m for the first vesicle and 178 mN/m for the second vesicle.

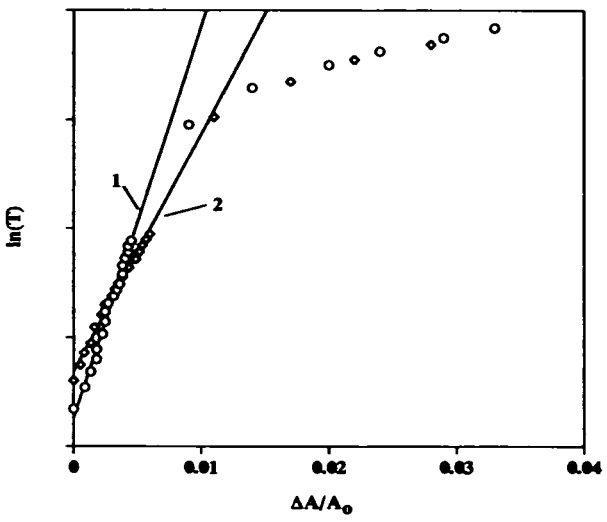

FIGURE 4 Log plot of the data shown in Fig. 3. The data for small suction pressures can be approximated with regression lines, and the slopes are 722 and 438 for the first and the second vesicle, respectively. The corresponding bending moduli are 1.1×10^{-19} and 0.7×10^{-19} J, respectively.

DISCUSSION

A new method is presented for measuring the bending modulus of lipid vesicles. The method is used to determine the bending modulus for SOPC bilayers. The bending modulus of the same bilayer is determined also by using a different method developed by Evans and Rawicz (1990), and it is shown that the values found by the two methods are similar. The proposed method, however, is not very sensitive for membranes with small bending moduli, compared with the other available methods. The advantage of this method will be in measuring the bending moduli for membranes having a large bending resistance when the amplitudes of the thermal fluctuations are small or for highly viscous membranes where the viscous dissipation in the plane of the membrane is significant (Duwe et al., 1990). This method also can be used to characterize the bending resistance of cell surfaces, where no other methods are available (Zhelev et al., 1993).

The analysis given here shows that the applied suction pressure in the small pipet for deforming the vesicle surface can be divided into two parts: 1) the suction pressure required to bend the vesicle membrane at zero membrane tension, and 2) the suction pressure required to deform the vesicle membrane when it has a constant tension and no bending rigidity. In Eq. 2, the first term gives the suction pressure for bending the membrane, and the second term gives the suction pressure that balances the tension in the membrane. (The second term is the formula for the "Law of Laplace.") A common feature in the experiments is that the pressure in the small pipet that is required for deformation of the vesicle membrane into a hemispherical shape (when flow begins) is larger than the pressure required to keep the vesicle aspirated into both pipets and in a state of metastable equilibrium (see Fig. 1 *A*). The geometry changes related to the initial vesicle deformation and to the partially aspirated vesicle show that during the initial deformation the curvature changes are much bigger than in the case when the vesicle is partially aspirated into both pipets. Then the free energy changes and the related suction pressures during the initial deformation in the small pipet are expected to be larger than the free energy changes and the suction pressure for metastable equilibrium. The difference between the two suction pressures for small membrane tensions can be used for a rough estimation of the bending modulus. In these experiments, the difference between the suction pressure for initial deformation and flow and the suction pressure for a partially aspirated vesicle in metastable equilibrium was on the order of the measured intercepts from the pressure-pressure plots shown in Fig. 2.

Another assumption made in the model is that the vesicle membrane tension is determined by setting the suction pressure in the large pipet. Our experiments show, however, that for small or zero suction pressures in the large pipet the relationship between the suction pressures in the two pipets is not linear. The deviation from linearity is a result of the existence of a membrane tension in the free vesicle membrane. We consider three sources of tension in the vesicle membrane beyond that produced by the holding pipet: thermal excitations, convection flow, and density differences. The membrane tensions caused by convection flows and density differences were not large enough to alter the thermal fluctuations of the vesicle membrane. We assume that the thermal excitations are the dominating factor determining the membrane tension of the free vesicle membrane. The effective tension in the vesicle membrane caused by thermal excitations is estimated to be in the order of 1.5×10^{-5} mN/m (Duwe et al., 1990: Faucon et al., 1989). The method proposed by Evans and Rawicz (1990) is based on this phenomena, and they have shown that the thermal fluctuations determine the membrane tensions up to $2–3 \times 10^{-3}$ mN/m. The membrane tension is affected by the thermal excitations for tensions up to 0.1 mN/m. Above this value, the dependence of the membrane tension on the fractional area change is linear (see Fig. 3), and it depends only on the area expansion modulus. The membrane tensions found from the measured suction pressures for flow of a free vesicle in the small pipet and for the escape of a vesicle from the large pipet are $2.8–3.9 \times 10^{-3}$ and $2.2–2.8 \times 10^{-3}$ mN/m, respectively. The experimental data shown in Fig. 2 indicate that the effect of thermal fluctuations is negligible for small pipet suction pressures above 30 Pa, which corresponds to an effective membrane tension of 8.5×10^{-3} mN/m. To minimize the effect of thermal fluctuations on the experimentally determined intercepts and slopes from the pressure-pressure plot in Fig. 2, only small pipet suction pressures above 30 Pa are used.

The accuracy of determining the bending modulus depends on the ability to measure precisely the suction pressures and the coefficients in Eq. 2. The suction pressures in the two pipets can be measured with an accuracy of 0.3–0.5 Pa, which gives about 10% error in the measured intercepts. The suction pressures are defined as a difference between the static pressure in the experimental chamber and the static pressure in the pipet (as measured by the movement of the reference reservoir). Because the experimental chamber is open, there is an air-water interface and the static pressure in the chamber depends on the curvature of this interface. The curvature of this interface depends on the amount of the solution in the chamber. In case of slow evaporation, the chamber static pressure (and the apparent suction pressure) can change at the rate of 1 Pa/min or more. Another effect of water evaporation is the osmolarity change. When the osmolarity of the solution in the chamber changes, the volume of the vesicle will change simultaneously and the measured suction pressures for vesicle flow at the beginning of the experiment and at the end (a typical experiment takes 5–10 min) for the same suction pressure in the large pipet will be different. Thus, the method must be used at the dew point for a given temperature and humidity, when the rate of evaporation and condensation are equal.

Measuring pipet diameters with the scanning electron microscope (SEM) is more accurate than using the light microscope, but even in this case the experimental error could

be in the order of 0.02 μm. The dependence of the bending modulus on the radius of the small pipet is shown in Fig. 5. The small pipet radius is varied between 0.54 and 0.62 μm, which is greater than the error of measuring the pipet radius from the SEM, and for this range of values the bending modulus changes about 25%.

The small torus radius of about 0.1 μm found from the slope in Fig. 2 and from Eq. 2 depends strongly on the small pipet radius, and we consider the error in its measurement as the largest source of error. Fig. 6 shows the dependence of the bending modulus when it is assumed that the small torus radius could vary from essentially zero to 1 μm. A radius greater than 0.5 μm could be seen with the light microscope. Such a large radius is not observed. It is seen that the bending modulus does not depend strongly on the small torus radius except for small radii. Another criteria for the value of the small torus radius can be found from minimum energy considerations. The spherical vesicle has the minimum bending energy equal to $8\pi k_c$. When the vesicle is deformed in the pipet, its bending energy increases. The intercept in Eq. 2 represents the increase of the total bending energy of the vesicle membrane when the projection length in the small pipet with radius R_{ps} changes from $(R_{ps} - dh)$ to R_{ps}. Thus, the shape of the vesicle will adjust in a way that the total free bending energy (or the increase of the free energy between two consecutive positions) will be minimum. All of the parameters in Eq. 2 except the small torus radius represent either the intrinsic properties of the membrane material (bending modulus) or the geometry imposed by the boundaries. Then another estimation for the small torus radius is found from the minimum of the increase of the free energy. Fig. 7 shows the dependence of the increase of the bending free energy on the small torus radius. The increase of the bending energy of the first and the second liposomes has minima at small torus radii equal to 0.4 and 0.35 μm, respectively. Using these values, estimates for the bending moduli can be found from the experimentally measured intercepts. The estimates are 1.15×10^{-19} and 1.08×10^{-19} J for the first and the second vesicle, respectively. This is in the same order of magnitude as the bending moduli found from Eq. 2 and the measured values for the slopes in Fig. 2.

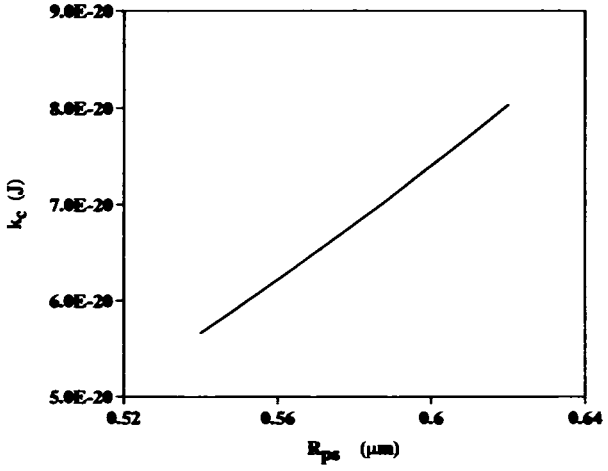

FIGURE 5 Dependence of the bending modulus k_c on the small pipet radius R_{ps}.

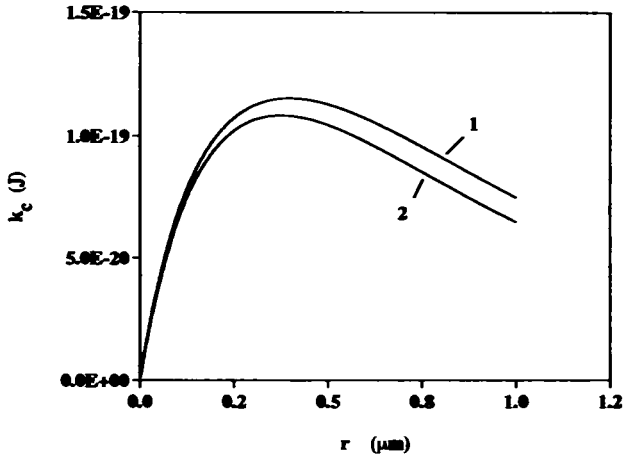

FIGURE 6 Dependence of the bending modulus k_c on the small torus radius r for the two vesicles studied in these experiments. Curve 1 is for the first vesicle, and curve 2 for the second one.

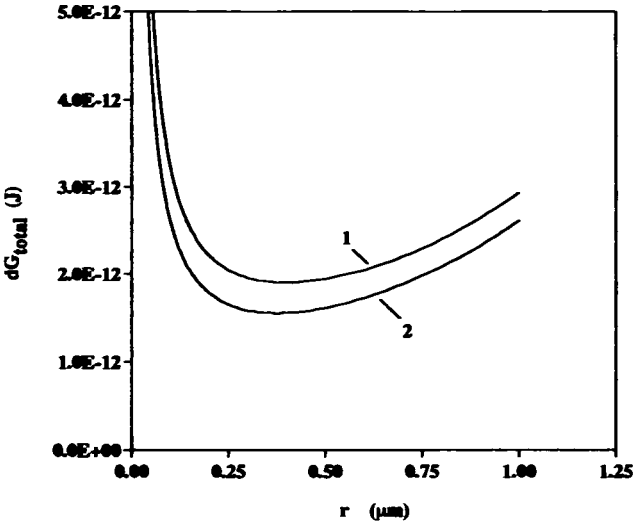

FIGURE 7 Dependence of the change of the vesicle total bending free energy dG_{total} on the small torus radius for the first (*curve 1*) and for the second (*curve 2*) vesicles.

In addition to the above sources of error, there is an error from deviation of the experimentally imposed boundary restrictions from the ones assumed in the model. There are two major factors that can influence the measured values of the bending modulus. The first one is the geometry of the pipet orifice. The pipet orifice is expected to seal perfectly the spherically shaped surface of the vesicle. However, this condition might not be met if the orifice is irregular. In some experiments (data not shown), the measured "apparent" values of the bending modulus are up to an order of magnitude larger than that found from the slope and intercept in Fig. 2.

When observed with the SEM, the orifices of the pipets in these experiments are not smooth. The second factor that leads to larger values of the "apparent" bending modulus than its "true" value is the distance between the two pipets. When the distance between the pipets is intentionally decreased, the values of the "apparent" bending modulus increase several times (data not shown) because the curvature of the outside region changes. These two factors lead to larger values of the "apparent" bending modulus than its "true" value. The result is that the measured values of the bending modulus are not normally distributed, and the "true" value is close to the minimum measured one (which for this work is represented by the values found from the data in Fig. 2). The values of the bending modulus in the literature found by different methods vary 2 to 3 times (Table I in Zhelev et al., 1994). The reason for this deviation is that the bending modulus is not a directly measurable parameter. For example, the bending modulus found from thermal fluctuations of tubular structures (Servuss et al., 1976) and large sheets (Mutz and Helfrich, 1990) can be affected by the presence of physical boundaries, which effectively is equivalent to an increased resistance for bending. Faucon et al. (1989) have shown that the larger values of the bending modulus, found by the thermal fluctuation method in the earlier experiments, are caused by the inability to measure precisely instantaneous positions. The values of the bending modulus determined from static methods (Evans and Rawicz, 1990; Waugh et al., 1992; and the method developed in this work) depend on the actual shape of the membrane surface at the pipet orifice (in the method of Waugh et al. (1992), it also depends on the geometry in the tether region), which is not a directly measurable parameter.

In conclusion, a new method for measuring the bending modulus of bilayer membranes is presented. Taking into account the deviation of the values of the bending modulus in the literature, the measured value for the SOPC membrane on the order of 0.6–1.15 $\times 10^{-19}$ J using this method, is in agreement with the value of 0.9 $\times 10^{-19}$ J measured by Evans and Rawicz (1990) and the value of 1.55 $\times 10^{-19}$ J given by Song and Waugh (1990) for the same type of bilayer membrane.

This work is supported by grant 2 RO1 HL23728 from the National Institutes of Health.

APPENDIX

The vesicle aspirated with the two pipets is divided into six regions, which are referred as: "s," the portion in the small pipet; "ts," the torus region in contact with the small pipet; "out," the spherical unbounded part of the vesicle; "tl," the torus region in contact with the large pipet; "cyl," the cylindrical region inside the large pipet; and "hl," the hemispherical cap inside the large pipet. Then the bending free energy for every one of the six regions is found from the definition (Eq. 1) and the specified geometry (Fig. 1 *B*).

Inside the small pipet the bending energy, G_s, is

$$G_s = \frac{\pi k_c}{2}(R_{ps}^2 + h^2)\left(\frac{4h}{R_{ps}^2 + h^2}\right)^2, \tag{A1}$$

where k_c is the bending modulus, R_{ps} is the radius of the small pipet, and $h < R_{ps}$ is the projection length of the vesicle inside the small pipet.

The bending energy of the torus region G_{ts} at the small pipet is

$$G_{ts} = \frac{k_c}{2}\int_{(-\pi)}^{(\pi)}\int_{((\pi/2)+\beta)}^{(\pi-\alpha)}\frac{1}{r}(R_{ts} + r\cos\nu)\left(2 - \frac{R_{ts}}{R_{ts} + r\cos\nu}\right)^2 d\nu\, d\varphi$$

$$= 4\pi k_c(\sin\alpha + \cos\beta) \tag{A2}$$

$$+ \frac{2\pi k_c R_{ts}}{r(1 - (r/R_{ts})^2)^{1/2}}\left(\tan^{-1}\left(\frac{C_{ts}\sin\alpha}{1 - \cos\alpha}\right) - \tan^{-1}\left(\frac{C_{ts}(1 + \sin\beta)}{\cos\beta}\right)\right),$$

where $-\pi \le \varphi \le \pi$ and $\pi - \alpha \le \nu \le (\pi/2) + \beta$, r is the small torus radius (see Fig. 1b), which is assumed to remain constant, $R_{ts} = R_{ps} + 2rhR_{ps}/(R_{ps}^2 + h^2)$ and $C_{ts} = ((1 - r/R_{ts})/(1 + r/R_{ts}))^{1/2}$.

The bending energy G_{out} of the outside spherical portion of the vesicle is

$$G_{out} = 4\pi k_c\left(\left(1 - \frac{R_{ts}^2}{(r + R_{out})^2}\right)^{1/2} + \left(1 - \frac{R_{tl}^2}{(r + R_{out})^2}\right)^{1/2}\right), \tag{A3}$$

where R_{out} is the radius of the outside vesicle region and $R_{tl} = R_{pl} + r$. In Eq. A3 and in Fig. 1, it is assumed for simplicity that the small torus radii at the two pipet orifices are equal ($r_s = r_l = r$).

The bending energy G_{tl} for the torus region at the large pipet is

$$G_{tl} = \frac{k_c}{2}\int_{(-\pi)}^{(\pi)}\int_{((\pi/2)+\gamma)}^{(\pi)}\frac{1}{r}(R_{tl} + r\cos\nu)\left(2 - \frac{R_{tl}}{R_{tl} + r\cos\nu}\right)^2 d\nu\, d\varphi \tag{A4}$$

$$= -4\pi k_c\cos\gamma - \frac{2\pi k_c R_{tl}}{r(1 - (r/R_{tl})^2)^{1/2}}\tan^{-1}\left(\frac{C_{tl}(1 + \sin\gamma)}{\cos\gamma}\right),$$

where $C_{tl} = ((1 - r/R_{tl})/(1 + r/R_{tl}))^{1/2}$.

The bending energy G_{cyl} of the cylindrical part inside the large pipet is

$$G_{cyl} = \frac{\pi k_c L}{R_{pl}}, \tag{A5}$$

where L is the length of the cylindrical region.

The bending energy G_{hl} of the hemispherical part inside the large pipet is

$$G_{hl} = 4\pi k_c. \tag{A6}$$

The change of the projection length dh inside the small pipet can be coupled with the changes of the outside vesicle radius dR_{out} and the projection length inside the large pipet dL by assuming that during this shape perturbation the volume and the area of the vesicle remain constant ($dS_{total} = 0$ and $dV_{total} = 0$). Therefore, the relationship between dh, dR_{out}, and dL, when $h \to R_{ps}$ is

$$dS_{total} = 0 = 2\pi(R_{ps} + r)\cdot dh + 2\pi R_{out}C_{vs}\cdot dR_{out} + 2\pi R_{pl}\cdot dL,$$
$$dV_{total} = 0 = \pi(R_{ps}^2 + rR_{ps}C_{vt})\cdot dh + \pi R_{out}^2 C_{vs}\cdot dR_{out} + \pi R_{pl}^2\cdot dL, \tag{A7}$$

where

$$C_{vt} = 1 + \left(\frac{R_{ps} + r}{R_{ps}}\right) + \left(\frac{R_{ps} + r}{R_{ps}}\right)^2$$

and

$$C_{vs} = \frac{2 - ((R_{ps} + r)/R_{out})^2}{(1 - ((R_{ps} + r)/R_{out})^2)^{1/2}} + \frac{2 - ((R_{pl} + r)/R_{out})^2}{(1 - ((R_{pl} + r)/R_{out}))^2)^{1/2}}.$$

In Eq. A7, it is assumed that the volume change in the torus region can be represented by the volume change of the truncated cone having the same radii and including the torus segment. Then from Eq. A7, the dependence of dR_{out} and dL on dh is

$$dR_{out} = \frac{R_{ps}(R_{pl} - R_{ps}) + r(R_{pl} - C_{vt}R_{ps})}{C_{vs}R_{out}(R_{out} - R_{pl})}\cdot dh,$$
$$dL = \frac{R_{ps}(R_{out} - R_{ps}) + r(R_{out} - C_{vt}R_{ps})}{R_{pl}(R_{out} - R_{pl})}\cdot dh. \tag{A8}$$

The change of the total bending energy is found as a sum of the changes of the bending energies for the six regions:

$$dG_{total} = dG_s + dG_{ts} + dG_{out} + dG_{cyl}. \quad (A9)$$

The bending energy of the hemispherical cap inside the large pipet G_{hl} is constant, and the change of the bending energy of the "tl" region dG_{tl} is negligible. These two terms are not included in Eq. A9. Then the change of the total bending energy, when $R_{out} \gg r$ and $h \to R_{ps}$, is

$$dG_{total} = \frac{\pi k_c (1 + r/R_{ps})^2 (1 + 2r/R_{ps})^{1/2}}{r} \cdot dh + \frac{4\pi k_c C_{ww}(R_{ps}(R_{pl} - R_{ps}) + r(R_{pl} - R_{ps}C_{vt}))}{C_{vs}R_{out}^2(R_{out} - R_{pl})} \cdot dh - \frac{\pi k_c (R_{ps}(R_{out} - R_{ps}) + r(R_{out} - R_{ps}C_{vt}))}{R_{pl}^2(R_{out} - R_{pl})} \cdot dh \quad (A10)$$

where

$$C_{ww} = \frac{((R_{ps} + r)/R_{out})^2}{(1 - ((R_{ps} + r)/R_{out})^2)^{1/2}} + \frac{((R_{pl} + r)/R_{out})^2}{(1 - ((R_{pl} + r)/R_{out})^2)^{1/2}}.$$

From the conservation of energy principle, the bending free energy change from Eq. A10 is equal to the work for displacing the vesicle boundaries in the six regions. The total work for the vesicle when the projection length inside the small pipet changes from h to $(h + dh)$ is,

$$dW_{total} = dW_s + dW_{ts} + dW_{out} + dW_{hl}. \quad (A11)$$

The work on the cylindrical region in the large pipet is zero, and the work in the torus region close to the large pipet is negligible. The work terms for the different regions in Eq. A11 are

$$\begin{aligned} dW_s &= \pi(P_{ves} - P_{sp})R_{ps}^2 \cdot dh, \\ dW_{ts} &= \pi(P_{ves} - P_{ch})rR_{ps}C_{vt} \cdot dh, \\ dW_{out} &= \pi(P_{ves} - P_{ch})R_{out}\frac{R_{ps}(R_{pl} - R_{ps}) + r(R_{pl} - C_{vt}R_{ps})}{(R_{out} - R_{pl})} \cdot dh, \\ dW_{hl} &= -\pi(P_{ves} - P_{lp})R_{pl}\frac{R_{ps}(R_{out} - R_{ps}) + r(R_{out} - C_{vt}R_{ps})}{(R_{out} - R_{pl})} \cdot dh, \end{aligned} \quad (A12)$$

where P_{ves} equals the pressure inside the vesicle, P_{sp} equals the pressure in the small pipet, P_{lp} equals the pressure in the large pipet and P_{ch} equals the pressure in the experimental chamber. Then the total work is

$$dW_{total} = \pi\left(R_{ps}^2\Delta P_s - \frac{R_{pl}(R_{ps}(R_{out} - R_{ps}) + r(R_{out} - C_{vt}R_{ps}))}{(R_{out} - R_{pl})}\Delta P_l\right) \cdot dh, \quad (A13)$$

where $\Delta P_s = (P_{ch} - P_{sp})$ and $\Delta P_l = (P_{ch} - P_{lp})$ are the experimentally measured pressure differences between the small pipet and the chamber and the large pipet and the chamber, respectively. From Eqs. A10 and A13, the relationship between the suction pressures of the two pipets is

$$\Delta P_s = f_0\left(\frac{R_{pl}}{R_{ps}}, \frac{R_{out}}{R_{ps}}, \frac{r}{R_{ps}}\right) \cdot \frac{k_c}{R_{ps}^3} + f_1\left(\frac{R_{pl}}{R_{ps}}, \frac{R_{out}}{R_{ps}}, \frac{r}{R_{ps}}\right) \cdot \frac{\Delta P_l}{R_{ps}}, \quad (A14)$$

where the functional coefficients are

$$f_0\left(\frac{R_{pl}}{R_{ps}}, \frac{R_{out}}{R_{ps}}, \frac{r}{R_{ps}}\right) = \frac{(1 + r/R_{ps})^2(1 + 2r/R_{ps})^{1/2}}{r/R_{ps}} + \frac{4C_{ww}((R_{pl}/R_{ps} - 1) + (r/R_{ps})(R_{pl}/R_{ps} - C_{vt}))}{C_{vs}(R_{out}/R_{ps})^2(R_{out}/R_{ps} - R_{pl}/R_{ps})} - \frac{((R_{out}/R_{ps} - 1) + (r/R_{ps})(R_{out}/R_{ps} - C_{vt}))}{(R_{pl}/R_{ps})^2(R_{out}/R_{ps} - R_{pl}/R_{ps})}$$

and

$$f_1\left(\frac{R_{pl}}{R_{ps}}, \frac{R_{out}}{R_{ps}}, \frac{r}{R_{ps}}\right) = \frac{(R_{pl}/R_{ps})((R_{out}/R_{ps} - 1) + (r/R_{ps})(R_{out}/R_{ps} - C_{vt}))}{(R_{out}/R_{ps} - R_{pl}/R_{ps})}.$$

REFERENCES

Duwe, H. P., J. Kaes, and E. Sackmann. 1990. Bending elastic moduli of lipid bilayers: modulation by solutes. *J. Phys. France.* 51:945–961.

Evans, E. A., and R. Skalak. 1980. Mechanics and Thermodynamics of Biomembranes. CRC Press Inc., Boca Raton, FL.

Evans, E. A., and W. Rawicz. 1990. Entropy-driven tension and bending elasticity in condensed-fluid membranes. *Phys. Rev. Lett.* 64:2094–2097.

Fancon, J. F., M. D. Mitov, P. Meleard, I. Bivas, and P. Bothorel. 1989. Bending elasticity and thermal fluctuations of lipid membranes. Theoretical and experimental requirements. *J. Phys. France.* 50:2389–2414.

Helfrich, W. 1973. Elastic properties of lipid bilayers: theory and possible experiments. *Z. Naturforsch.* 28c:693–703.

Kwok, R., and E. A. Evans. 1981. Thermoelasticity of large lecithin bilayer vesicles. *Biophys. J.* 35:637–652.

Milner, S. T., and S. A. Safran. 1987. Dynamical fluctuations of droplet microemulsions and vesicles. *Phys. Rev. A.* 36:4371–4379.

Mutz, M., and W. Helfrich. 1990. Bending rigidities of some biological model membranes as obtained from the fourier analysis of contour sections. *J. Phys. France.* 51:991–1002.

Schneider, M. B., J. T. Jenkins, and W. W. Webb. 1984a. Thermal fluctuations of large cylindrical phospholipid vesicles. *Biophys. J.* 45: 891–899.

Schneider, M. B., J. T. Jenkins, and W. W. Webb. 1984b. Thermal fluctuations of large quasi-spherical bimolecular phospholipid vesicles. *J. Physique.* 45:1457–1472.

Servuss, R. M., W. Harbich, and W. Helfrich. 1976. Measurement of the curvature-elastic modulus of egg lecithin bilayers. *Biochim. Biophys. Acta.* 436:900–903.

Song, J., and R. E. Waugh. 1990. Bilayer membrane bending stiffness by tether formation from mixed PC-PS lipid vesicles. *J. Biomech. Eng.* 112: 235–240.

Waugh, R. E., J. Song, S. Svetina, and B. Zeks. 1992. Local and nonlocal curvature elasticity in bilayer membranes by tether formation from lecithin vesicles. *Biophys. J.* 61:974–982.

Zhelev, D. V., D. Needham, and R. M. Hochmuth. 1994. Role of the membrane cortex in neutrophil deformation in small pipets. *Biophys. J.* 67: 696–705.